



Amnis® Imaging Flow Cytometry
Integrating flow cytometry and
microscopy to advance discovery

EMD Millipore is a division of Merck KGaA, Darmstadt, Germany



Globosides but Not Isoglobosides Can Impact the Development of Invariant NKT Cells and Their Interaction with Dendritic Cells

This information is current as of January 8, 2013.

Stefan Porubsky, Anneliese O. Speak, Mariolina Salio, Richard Jennemann, Mahnaz Bonrouhi, Rashad Zafarulla, Yogesh Singh, Julian Dyson, Bruno Luckow, Agnes Lehuen, Ernst Malle, Johannes Müthing, Frances M. Platt, Vincenzo Cerundolo and Hermann-Josef Gröne

J Immunol 2012; 189:3007-3017; Prepublished online 8 August 2012;

doi: 10.4049/jimmunol.1201483

<http://www.jimmunol.org/content/189/6/3007>

Supplementary Material <http://www.jimmunol.org/content/suppl/2012/08/08/jimmunol.1201483.DC1.html>

References This article **cites 74 articles**, 36 of which you can access for free at: <http://www.jimmunol.org/content/189/6/3007.full#ref-list-1>

Subscriptions Information about subscribing to *The Journal of Immunology* is online at: <http://jimmunol.org/subscriptions>

Permissions Submit copyright permission requests at: <http://www.aai.org/ji/copyright.html>

Email Alerts Receive free email-alerts when new articles cite this article. Sign up at: <http://jimmunol.org/cgi/alerts/etoc>

The Journal of Immunology is published twice each month by
The American Association of Immunologists, Inc.,
9650 Rockville Pike, Bethesda, MD 20814-3994.
Copyright © 2012 by The American Association of
Immunologists, Inc. All rights reserved.
Print ISSN: 0022-1767 Online ISSN: 1550-6606.



Globosides but Not Isoglobosides Can Impact the Development of Invariant NKT Cells and Their Interaction with Dendritic Cells

Stefan Porubsky,^{*,†} Anneliese O. Speak,[‡] Mariolina Salio,[§] Richard Jennemann,^{*} Mahnaz Bonrouhi,^{*} Rashad Zafarulla,[¶] Yogesh Singh,[¶] Julian Dyson,[¶] Bruno Luckow,^{||} Agnes Lehuen,[#] Ernst Malle,^{**} Johannes Müthing,^{††} Frances M. Platt,[‡] Vincenzo Cerundolo,[§] and Hermann-Josef Gröne^{*}

Recognition of endogenous lipid Ag(s) on CD1d is required for the development of invariant NKT (iNKT) cells. Isoglobotrihexosylceramide (iGb3) has been implicated as this endogenous selecting ligand and recently suggested to control overstimulation and deletion of iNKT cells in α -galactosidase A-deficient (α Gala^{-/-}) mice (human Fabry disease), which accumulate isoglobosides and globosides. However, the presence and function of iGb3 in murine thymus remained controversial. In this study, we generate a globotrihexosylceramide (Gb3)-synthase-deficient (*Gb3S*^{-/-}) mouse and show that in thymi of α Gala^{-/-}/*Gb3S*^{-/-} double-knockout mice, which store isoglobosides but no globosides, minute amounts of iGb3 can be detected by HPLC. Furthermore, we demonstrate that iGb3 deficiency does not only fail to impact selection of iNKT cells, in terms of frequency and absolute numbers, but also does not alter the distribution of the TCR CDR 3 of iNKT cells. Analyzing multiple gene-targeted mouse strains, we demonstrate that globoside, rather than iGb3, storage is the major cause for reduced iNKT cell frequencies and defective Ag presentation in α Gala^{-/-} mice. Finally, we show that correction of globoside storage in α Gala^{-/-} mice by crossing them with *Gb3S*^{-/-} normalizes iNKT cell frequencies and dendritic cell (DC) function. We conclude that, although detectable in murine thymus in α Gala^{-/-}/*Gb3S*^{-/-} mice, iGb3 does not influence either the development of iNKT cells or their interaction with peripheral DCs. Moreover, in α Gala^{-/-} mice, it is the Gb3 storage that is responsible for the decreased iNKT cell numbers and impeded Ag presentation on DCs. *The Journal of Immunology*, 2012, 189: 3007–3017.

Natural killer T cells represent a discrete T cell population expressing TCR $\alpha\beta$ together with NK cell surface markers such as NK1.1 (CD161) (1). A subset of NKT

cells expresses an invariant TCR α -chain (V α 14-J α 18 in mouse and V α 24-J α 18 in human) with a restricted set of TCR β -chains (V β 2, V β 7, and V β 8.2 in mouse and V β 11 in human) and is thus referred to as invariant NKT (iNKT or type I NKT) cells (2–5). Although constituting <1% of mouse lymphocytes, iNKT cells have repeatedly been shown to play an important role in tumor surveillance, in establishing peripheral tolerance, and also in defense against infections (6–10).

Unlike MHC class I (MHC I)- and II (MHC II)-restricted T cells, iNKT cells recognize exogenous and endogenous lipid Ags presented by nonpolymorphic MHC I-like CD1 molecules (11, 12). Several exogenous microbial lipid and glycolipid Ags recognized by iNKT cells have been identified (13, 14). The prototypical iNKT cell agonist is α -galactosylceramide (α GalCer, also referred to as KR7000), a glycosphingolipid (GSL), which is derived from the marine sponge *Agelas mauritanicus* (15, 16). α GalCer represents a specific and strong ligand for iNKT cells eliciting a rapid release of Th1- and Th2-type cytokines in large amounts.

Although conventional T cells require presentation of peptide Ags on MHC I or II molecules of cortical epithelial cells, positive selection of iNKT cells requires the presentation of an endogenous lipid Ag by CD1 molecules of double-positive (CD4⁺/CD8⁺) cortical thymocytes (17). CD1d deletion or aberrant trafficking due to a mutation in its cytoplasmic tail interferes with the positive thymic selection of iNKT cells with the consequence of diminished iNKT cell numbers (18, 19). Nevertheless, CD1 molecules alone are not sufficient for the positive selection of iNKT cells, because sphingolipid activator proteins and lysosomal proteases are also indispensable for normal iNKT cell selection (20, 21), suggesting that a lipid self-Ag(s) is loaded onto CD1 to enable

*Department of Cellular and Molecular Pathology, German Cancer Research Center, 69120 Heidelberg, Germany; †Institute of Pathology, University Medical Center Mannheim, University of Heidelberg, 68167 Mannheim, Germany; ‡Department of Pharmacology, University of Oxford, Oxford OX1 3QT, United Kingdom; §Medical Research Council Human Immunology Unit, Weatherall Institute of Molecular Medicine, John Radcliffe Hospital, Oxford OX3 9DS, United Kingdom; ¶Section of Immunobiology, Department of Medicine, Imperial College London, London SW7 2AZ, United Kingdom; ||Klinikum der Universität München, Medizinische Klinik und Poliklinik IV, Nephrologisches Zentrum, Arbeitsgruppe Klinische Biochemie, 80336 Munich, Germany; #INSERM Unité 986, Hôpital Cochin/St. Vincent de Paul, 75014 Paris, France; **Institute of Molecular Biology and Biochemistry, Center for Molecular Medicine, Medical University of Graz, 8010 Graz, Austria; and ††Institute for Hygiene, University of Münster, 48149 Münster, Germany

Received for publication May 31, 2012. Accepted for publication July 11, 2012.

This work was supported by grants from the Deutsche Forschungsgemeinschaft (to H.-J.G. and S.P.) (SFB 938). A.O.S. was supported by the Medical Research Council (U.K.) (G0700851). V.C. and M.S. were supported by Cancer Research (U.K.) (C399/A2291), the U.K. Medical Research Council, and the Wellcome Trust (084923/Z/08/Z).

Address correspondence and reprint requests to Dr. Hermann-Josef Gröne and Dr. Stefan Porubsky, Department of Cellular and Molecular Pathology, German Cancer Research Center, Im Neuenheimer Feld 280, 69120 Heidelberg, Germany. E-mail addresses: h.-j.groene@dkfz.de (H.-J.G.) and s.porubsky@dkfz.de (S.P.)

The online version of this article contains supplemental material.

Abbreviations used in this article: AcLDL, acetylated low-density lipoprotein; BMDC, bone marrow-derived dendritic cell; DC, dendritic cell; DCE, dichloroethane; α Gala^{-/-}, α -galactosidase A-deficient; α GalCer, α -galactosylceramide; Gb3, globotrihexosylceramide; *Gb3S*^{-/-}, globotrihexosylceramide-synthase-deficient; GlcCer, glucosylceramide; GSL, glycosphingolipid; iGb3, isoglobotrihexosylceramide; *iGb3S*^{-/-}, isoglobotrihexosylceramide-synthase-deficient; iNKT, invariant NKT; MHC I, MHC class I; MHC II, MHC class II; WT, wild-type.

Copyright © 2012 by The American Association of Immunologists, Inc. 0022-1767/12/\$16.00

positive selection of iNKT cells (12, 22). On the basis of the amino acid sequence, the five members of the human CD1 family have been assigned to either group I, which comprises CD1a, -b, -c, and -e molecules, or group II, which consists of the CD1d molecule. Unlike humans, mice lack group I CD1 molecules and have two group II *Cd1* genes termed *Cd1d1* and *Cd1d2*, from which only *Cd1d1* seems to encode for a functional protein (23). A variety of endogenous lipids have been demonstrated to be captured by CD1d on the secretory pathway or during endosomal-lysosomal recycling (22), the majority of them being phospholipids (including diacyl- and lyso-species, cardiolipins, and plasmalogens) or sphingolipids (sphingomyelin and glycosphingolipids) (24–27). However, most iNKT cells do not respond to these lipids, and the reactivity toward them is restricted to singular iNKT cell clones (28).

On the basis of the observation that cells deficient in glucosylceramide (GlcCer) based GSL (Fig. 1) are unable to stimulate iNKT cell hybridomas, it was suggested that the endogenous selecting ligand might be a GSL (29). Reduced iNKT cell numbers in mice deficient in the β -subunit of β -hexosaminidase (*Hexb*^{-/-}, Sandhoff storage disease; Fig. 1) together with the well documented in vitro stimulatory capacity of isoglobotrihexosylceramide (iGb3) toward iNKT cells led to the conclusion that iGb3 is the endogenous lipid ligand responsible for the positive selection of iNKT cells (30, 31). However, previously, we demonstrated that iGb3-synthase-deficient (*iGb3S*^{-/-}) mice have normal iNKT cell numbers and do not show a functional phenotype (32), suggesting that iGb3 is unlikely to be the only endogenous iNKT cell lipid ligand. Also, the presence of isoglobosides and iGb3 in murine thymus remains highly controversial: mass spectrometry showed the presence of iGb3 in murine thymus (33), whereas a highly sensitive HPLC failed to detect the iGb3 in the murine thymus, a possible

reason for this being that the major globotrihexosylceramide (Gb3) peak masked the putatively very low levels of iGb3 (34). Recently, it has been demonstrated that peroxisomal ether-bonded mono-alkyl glycerophosphates are potent activators of iNKT cells and that mice with absence of glyceronephosphate *O*-acyltransferase, the enzyme generating these lipids, show an altered thymic iNKT cell development (35).

Recognition of endogenous lipid Ags is also important for the function of peripheral iNKT cells, which are, however, capable of indirect activation without the need for recognition of CD1d-presented microbial lipid Ags (36). According to this concept, iNKT cell activation is mediated by upregulation and presentation of endogenous lipid Ags on CD1d upon recognition of microbial danger signals by APCs, in concert with cytokines such as IL-12 (37, 38). Even in this setting, the identity of the endogenous lipid (s) has not been fully elucidated. iGb3 was originally implicated in iNKT cell activation by TLR ligand-activated dendritic cells (DCs) (39), and it has been argued that in α -galactosidase A-deficient mice (*α GalA*^{-/-}, Fabry lysosomal storage disease; Fig. 1) iGb3 accumulation is responsible for overstimulation and decreased numbers of peripheral iNKT cells (40). However, more recently, GlcCer has been proposed as a relevant endogenous lipid Ag-mediating iNKT cell activation in response to microbial danger signals (41).

In the current study, we have generated Gb3-synthase-deficient (*Gb3S*^{-/-}) mice and used them in combination with *α GalA*^{-/-} storage mice, which enabled the accumulation of isoglobosides without globosides (Fig. 1). This allowed us to detect minute amounts of iGb3 in thymi of *α GalA*^{-/-}/*Gb3S*^{-/-} mice. In view of this finding, we reanalyzed in detail the TCR repertoire of iNKT cells developing (in normal frequencies) in *iGb3S*^{-/-} mice and demonstrated that they express a typical iNKT TCR repertoire

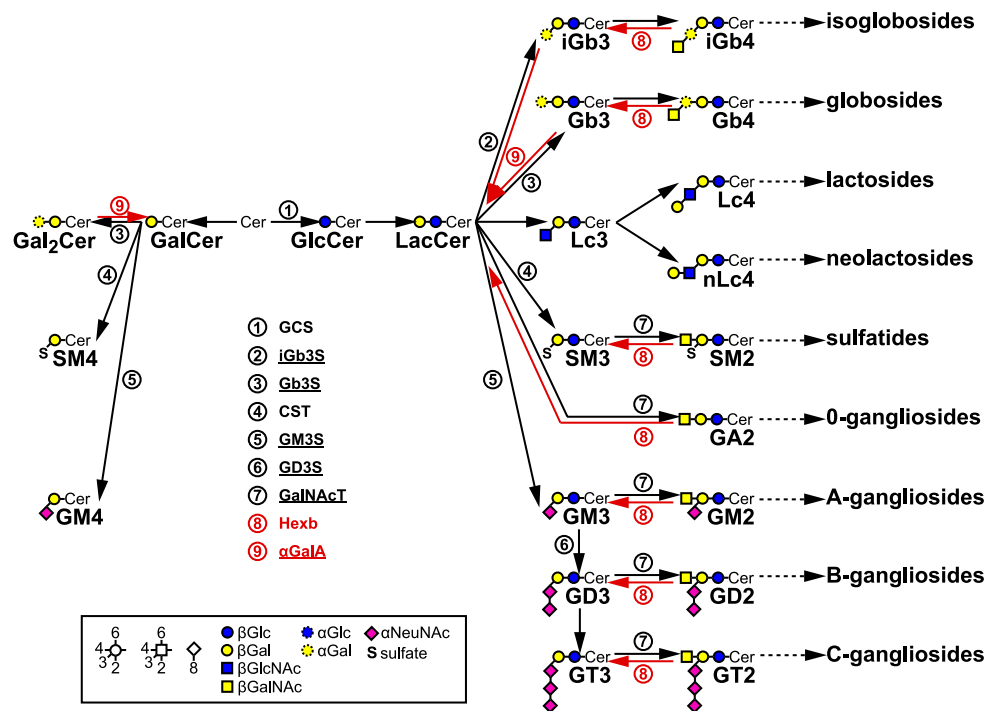


FIGURE 1. Metabolic GSL pathways. Shown are the most prominent mammalian groups of GSL with the two principal branches of GSL, which are based either on GalCer or GlcCer. GlcCer is invariably processed to lactosylceramide (LacCer). By subsequent action of further enzymes on either GalCer or LacCer, individual groups of GSL emerge, of which the most important are displayed. Relevant synthesis (black) and degradation (red) enzymes are indicated as encircled numbers: 1, GlcCer synthase (GCS); 2, iGb3 synthase (iGb3S); 3, Gb3 synthase (Gb3S); 4, cerebroside sulfotransferase (CST); 5, GM3 synthase (GM3S); 6, GD3 synthase (GD3S); 7, GalNAc transferase (GalNAcT); 8, β -hexosaminidase (Hexb); and 9, α -galactosidase A (α GalA). Enzymes investigated in this study are underlined.

Moreover, comparison of $\alpha\text{GalA}^{-/-}/\text{Gb3S}^{-/-}$ and $\alpha\text{GalA}^{-/-}/i\text{Gb3S}^{-/-}$ mice showed that it is not the accumulation of iGb3 but rather the storage of globosides that is responsible for the decreased iNKT cell numbers and altered Ag presentation on DCs in $\alpha\text{GalA}^{-/-}$ storage mice. This study shows, therefore, that despite its presence in thymus, iGb3 does not mediate the positive selection of iNKT cells, and neither is it the endogenous ligand responsible for the interaction between DCs and iNKT cells in the periphery.

Materials and Methods

Generation of $\text{Gb3S}^{-/-}$ mice

Clone MPMGc121J18724Q5 from the 129/Ola mouse genomic cosmid library number 121 from the German Resource Center for Genome Research (Berlin, Germany) containing the *Gb3S* (A4galt, EC 2.4.1.228) locus was used to construct a targeting vector by Red/ET homologous recombination technology (Gene Bridges, Dresden, Germany) (42). First, a 9.9-kb fragment corresponding to the region from 83,054,060 to 83,063,963 on chromosome 15 (National Center for Biotechnology Information m37 assembly) and bearing the *Gb3S* gene was subcloned into the plasmid vector pBluescript M13⁺ (Stratagene, Heidelberg, Germany). The coding sequence of exon 3 was then replaced by a loxP-flanked neomycin selection cassette (loxP-PGK-gb2-neo-loxP cassette; Gene Bridges). The deleted *Gb3S* sequences extended from position 83,057,694 to 83,059,066 (Fig. 2A). The targeting vector was electroporated into E14 embryonic stem cells, and 384 G418-resistant clones were picked, expanded, and characterized by Southern blot analysis using the 3'- and 5'-external probes (Fig. 2B), which had been generated by PCR using the following primers: 5'-CAG GCT GAA TGA CCT AAG GC-3'; 5'-GCT GCT TGT CTT CTG CGA C-3'; 5'-GAA CTC ACC CCA TCC AAG C-3'; and 5'-TGG TCA TAG TGC TCT AAG C-3', respectively. Two positive ES cell clones were detected and microinjected into C57BL/6 blastocysts. For Cre-mediated deletion of the loxP-flanked neomycin selection cassette, $\text{Gb3S}^{-/-}$ mice were crossed with a Cre deleter strain (43). Deletion of the selection cassette was proven by PCR using the primers F2 5'-GCT TCT GAC TGC CCT TTC AC-3' and R2 5'-TCC TTC TCC CTC AGC ATT TC-3' (2048 bp before and 498 bp after deletion; Fig. 2C). Mice were backcrossed for 10 generations to C57BL/6 (Charles River Wiga, Sulzfeld, Germany) prior to analysis.

Other genetically modified mice

Mice deficient for *iGb3S* (A3galt2^{tm1.1Hig}, EC 2.4.1.87) were generated by our group and backcrossed for >10 generations to the C57BL/6 genetic background (32). Mice deficient for GalNAc-transferase (B4galnt1, EC 2.4.1.92 (44)), GM3-synthase (St3gal5, EC 2.4.99.9 (45)), and GD3-synthase (St8sia1, EC 2.4.99.8 (46)) were provided by R. Proia (National Institutes of Health, Bethesda, MD); mice deficient for αGalA (EC 3.2.1.22) were provided by A. Kulkarni (National Institutes of Health) (47); TCRV α 14-J α 281 transgenic mice were donated by A. Lehuen (INSERM Unité 986, Hôpital Cochin/St. Vincent de Paul, Paris, France) (48). Cd1d1-deficient mice (49) were purchased from The Jackson Laboratory (Bar Harbor, ME). MyD88-deficient mice (50) were from Oriental BioService (Kyoto, Japan). All strains were housed under specific pathogen-free conditions. All animal experiments were performed in compliance with the German guidelines on animal protection and were approved by the local authority.

Organ preparation and flow cytometry

Single-cell preparations from organs were prepared as described previously (32). αGalCer -loaded PE-labeled CD1d tetramers were purchased from ProImmune (Oxford, U.K.). PBS57-loaded PE-labeled CD1d tetramers were provided by National Institutes of Health Tetramer Core Facility at Emory University (Atlanta, GA). Flow cytometry was performed as previously described (32) using the following mAbs: anti-CD1d (clone 1B1; BD, Heidelberg, Germany); anti-CD3e (145-2C11), anti-CD11c (HL3), anti-CD19 (MB19-1), anti-CD44 (IM7), and anti-MHCII (M5/144.15.2) (all from eBioscience, San Diego, CA); anti-Gb3 (CD77, 38-13) in combination with anti-rat IgM (both from GenTex, Irvine, CA). Analysis of flow cytometry data were performed using Cell Quest Pro software (BD) by gating on lymphocytes in the forward and side scatter.

In vitro experiments with DCs and iNKT cells

DCs were isolated from spleens by anti-CD11c microbeads (Miltenyi Biotec, Bergisch Gladbach, Germany) and plated at 50,000/well in 100 μl

medium (RPMI 1640 with 10% FCS, 1% penicillin/streptomycin, 1% glutamine, 1% nonessential amino acids, 1% sodium pyruvate, and 1% HEPES) in 96-well plates (Greiner Bio-One, Frickenhausen, Germany). αGalCer (Avanti Polar Lipids, Alabaster, AL) was applied overnight followed by thorough washing. Heat-killed *Escherichia coli* were prepared from overnight cultures by exposure to 70°C for 2 h and applied overnight on DCs at a bacteria/DC ratio of 10:1 followed by thorough washing. iNKT cells were enriched from livers of TCRV α 14-J α 281 transgenic mice using anti-CD5 micro beads (Miltenyi Biotec) and applied at 50,000/well in 100 μl medium as above. IFN- γ was measured by cytometric bead array technique (BD) after coincubating DCs and iNKT cells for 24 h in case of αGalCer presentation or 5 d in case that the interaction with DCs stimulated with heat-killed bacteria was assessed. OVA presentation toward MHC I- and II-restricted T cell hybridomas was tested as described previously (51). For cellular cholesterol/cholesteryl ester loading experiments, bone marrow-derived DCs (BMDCs) were prepared as described previously (51). Cells were incubated with 50 $\mu\text{g}/\text{ml}$ acetylated low-density lipoprotein (AcLDL) overnight followed by thorough washing. AcLDL was prepared following treatment of native LDL isolated as previously described (52) by multiple 2- μl aliquots of acetic anhydride (53).

Spectratyping

Thymic iNKT cells were enriched using 2 μl PBS57-loaded PE-labeled CD1d tetramers (National Institutes of Health Tetramer Core Facility at Emory University) in a total volume of 200 μl PBS with 1% BSA and 2 mM EDTA at room temperature for 30 min. After washing, the cell pellet was incubated with 10 μl anti-PE microbeads (Miltenyi Biotec) at 4°C for 15 min. Enrichment was performed according to the manufacturer's instruction using MS columns (Miltenyi Biotec). RNA was isolated using the acid phenol/chloroform extraction method (54). Contaminating genomic DNA was removed by digestion with RNase-free DNaseI (turbo DNA free; Ambion, Huntingdon, U.K.). The total amount of RNA was subjected to reverse transcription in a 20- μl volume using SuperscriptII (Invitrogen, Karlsruhe, Germany), according to the manufacturer's instructions. For TCR sequencing, V α 14 and V β 8.2 rearrangements were amplified using V α 14/C α (5'-TCC TGG TTG ACC AAA AAG AC-3' and 5'-CTT TCA GCA GGA GGA TTC G-3') and V β 8.2/C β (5'-GGT GAC ATT GAG CTG TAA T-3' and 5'-AGA AGC CCC TGG CCA AGC ACA-3') primers, respectively. PCR products were cloned using the TA Cloning kit (Invitrogen Life Technologies) and sequenced using the M13R primer. Spectratyping was performed as described using V β 2, 7, and 8.2 primers in combination with C β or J β primers (55).

HPLC

Glycolipid extraction, purification, ceramide glycanase digestion, and fluorescent derivatization were performed as described previously (34). Normal-phase HPLC was as previously described (34) with the exception that fluorescent detection was performed with a Waters 2475 detector (Waters, Milford, MA). Oligosaccharide standards for calibration were purchased from Dextra laboratories (Reading, U.K.). Green coffee bean α -galactosidase (α 1-3, 4, and 6) was purchased from Glyko Prozyme (Hayward, CA), and 50 mU was used per digest for 48 h with samples prepared for HPLC as described previously (34).

Isolation of neutral GSL

Freshly harvested spleens and kidneys were frozen in liquid nitrogen and lyophilized. Tissues were powdered, and dry weight was determined. GSL were extracted with 2 ml $\text{CHCl}_3/\text{CH}_3\text{OH}/\text{H}_2\text{O}$ 10:10:10 v/v/v under sonication in a water bath at 50°C for 15 min. After centrifugation at 4000 rpm for 10 min, supernatants were collected, and the pellets were extracted again first with 2 ml $\text{CHCl}_3/\text{CH}_3\text{OH}/\text{H}_2\text{O}$ (10:10:10, v/v/v) and then with $\text{CHCl}_3/\text{CH}_3\text{OH}/\text{H}_2\text{O}$ (30:60:8, v/v/v). Supernatants were combined and dried under a stream of air. Crude extracts were treated with 1 ml 0.1 M KOH in CH_3OH at 50°C for 4 h to eliminate phospholipids and triglycerides. After neutralization with acetic acid and evaporation of CH_3OH , potassium acetate was removed from lipids via reversed-phase column chromatography (RP18): small glass pipettes were filled with 200 μl silicagel RP18 material (Waters) preconditioned with 2 ml each of CH_3OH , H_2O , and 0.1 M potassium acetate in H_2O . Lipid extracts were suspended in 1 ml H_2O and applied to the columns. After washing with 4 ml H_2O , lipids were eluted with 4 ml methanol and dried. For the separation of GSL into neutral and acidic (sialic acid-containing) components by ion exchange chromatography, glass pipettes were filled with 200 μl DEAE Sephadex A25 (GE Healthcare, Uppsala, Sweden). Columns were preconditioned with 2 ml CH_3OH . The lipid extracts were solved in 2 ml CH_3OH and applied to the columns. Flow throughs containing neutral GSL

were collected. Neutral GSL were eluted from the columns with additional 4 ml CH₃OH and acidic GSL with 2 ml 0.5 M potassium acetate in CH₃OH. Neutral GSL were thoroughly dried and kept for several hours in a vacuum desiccator. GSL were solved in 200 μ l dichloroethane (DCE) and acetylated by the addition of 50 μ l acetic anhydride and 50 μ l 0.1% dimethylaminopyridine in DCE at 37°C for 1 h. The reaction solvents were evaporated under a N₂ stream by the addition of 200 μ l toluene, three times. Glass pipettes were filled with 400 μ l Florisil (Merck, Darmstadt, Germany) and washed with 4 ml DCE/*n*-hexane (4:1, v/v). The acetylated neutral GSL were solved in the same solvent mixture and applied to the columns followed by washing steps with DCE/*n*-hexane (4:1, v/v) and DCE, 4 ml each. GSL were eluted from columns with 4 ml DCE/acetone (1:1, v/v) and dried. To remove acetyl groups from sugar moieties, neutral GSL were solved in 0.1 M KOH in CH₃OH and incubated at 37°C for 2 h. After neutralization with acetic acid, the purified neutral GSL were dried and desalted by RP18 column chromatography as described above.

Thin layer chromatography

Neutral GSL were isolated from kidneys and spleens. An amount corresponding to 2 mg dry organ weight was loaded twice on two halves of a TLC plate (Merck). Running solvent was CHCl₃/CH₃OH/H₂O (62.5:30:6, v/v/v). The TLC plate was divided into two halves, and one part was sprayed with 0.2% orcinol in 10% sulfuric acid at 120°C for 10 min to visualize the GSL. The second part was used for anti-Gb3 immunostaining. For this purpose, the silicagel layer was fixed by dipping into a solution of 5% polyisobutylmethacrylate in CHCl₃ diluted 1:10 with *n*-hexane for 2 min. The plate was then dried for 10 min, and unspecific binding was blocked with 1% BSA in PBS for 1 h at room temperature. Polyclonal chicken anti-Gb3 Ab JM06/298-1 (56) was diluted 1:1000 in 1% BSA in PBS, and the plate was incubated overnight at 4°C. After intense washing with 0.05% Tween20 in PBS, alkaline phosphatase-conjugated polyclonal donkey anti-chicken IgY secondary Ab (Jackson ImmunoResearch Europe, Suffolk, U.K.) diluted 1:200 in 1% BSA in PBS was applied for 3 h at room temperature. Gb3 was visualized after a repeated washing step with 5-bromo-4-chloro-3-indolyl phosphate (Sigma-Aldrich, Munich, Germany) for 5 min at room temperature.

Electron microscopy

Organs were fixed in Karnovsky's glutaraldehyde (2% paraformaldehyde, 2.5% glutaraldehyde, and 0.2M cacodylate buffer [pH 7.4]) and embedded in araldite (Serva, Heidelberg, Germany). Ultrathin sections were stained with lead citrate and uranyl acetate. Photographs were taken on an electron microscope (Zeiss EM 910; Carl Zeiss, Oberkochen, Germany).

Statistical analysis

Unpaired two-tailed Student *t* test was performed to compare data sets. Differences were considered significant if *p* < 0.05. Numbers of independent observations per group are indicated for each result.

Results

iGb3 is present in extremely low amounts in the murine thymus

Using a highly sensitive HPLC method, we previously investigated the presence of isoglobosides, in particular *iGb3*, in various murine tissues (34). Despite the high sensitivity of this method, the only murine tissue with detectable *iGb3* levels was the dorsal root ganglion. *iGb3* was not detected in the thymus in either wild-type (WT) or α *Gala*^{-/-} mice (murine model of Fabry lysosomal storage disease) in which accumulation of isoglobosides—together with globosides—was expected (Fig. 1). However, the *iGb3* peak might have remained undetected because of overlap with the more abundant Gb3 peak.

Therefore, to circumvent this obstacle, we have now generated *Gb3S*^{-/-} mice (Fig. 2). TLC of kidney extracts, which are rich in globosides in WT mice, showed absence of Gb3 and its derivatives such as Gb4 in *Gb3S*^{-/-} mice, thereby demonstrating the successful targeted inactivation of the *Gb3S* gene (Fig. 2D).

Using the HPLC method previously reported (34), no *iGb3* could be detected in the thymus of *Gb3S*^{-/-} mice despite the absence of Gb3 (Fig. 3A); however, there was still a peak that comigrated with Gb3 and had a neutral charge in the *Gb3S*^{-/-} and is as yet unidentified. To increase the amounts of *iGb3* present in tissues yet without Gb3 accumulation, α *Gala*^{-/-} mice were crossed with *Gb3S*^{-/-} mice to promote the storage of *iGb3* if present. By this approach, a minute peak at the level of the *iGb3* standard could be detected in α *Gala*^{-/-}/*Gb3S*^{-/-} mice (Fig. 3B). Consistent with it being *iGb3*, this peak was also susceptible to α -galactosidase digestion (Fig. 3C) and was absent in triple α *Gala*^{-/-}/*Gb3S*^{-/-}/*iGb3S*^{-/-} knockout mice (Fig. 3D). Taking into account the number of thymocytes processed for this analysis, this peak detected in α *Gala*^{-/-}/*Gb3S*^{-/-} mice corresponded to

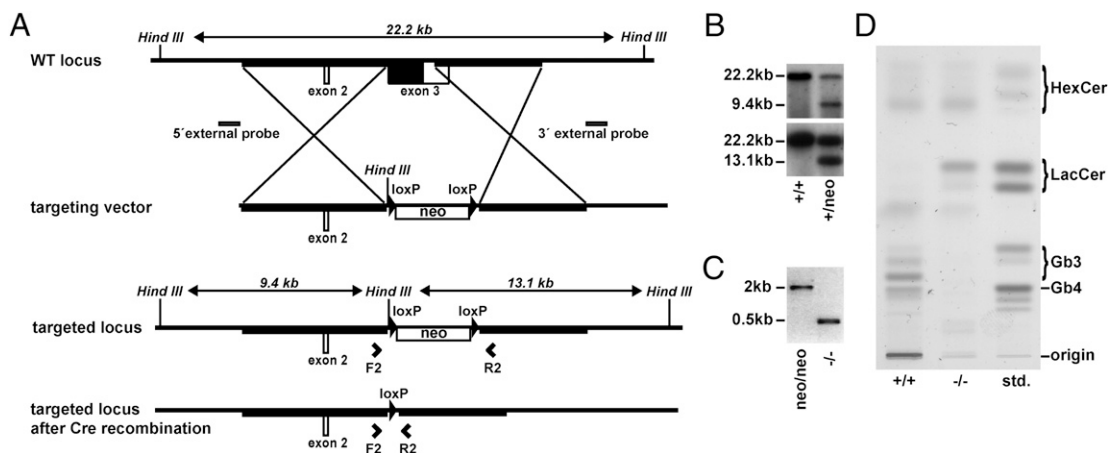
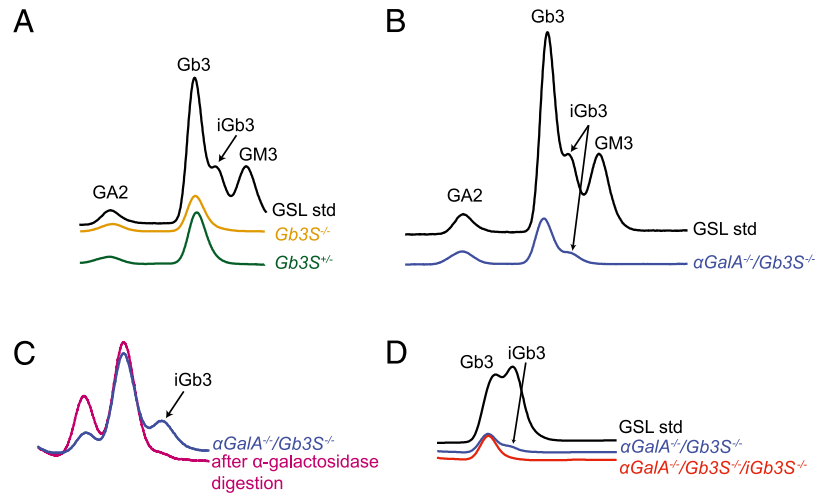


FIGURE 2. Generation of *Gb3S*^{-/-} mice. **(A)** Targeting strategy showing murine *Gb3S* WT locus, targeting vector, and the targeted locus before and after Cre-mediated recombination together with HindIII restriction sites and probes for Southern blot analysis. Coding and noncoding regions of exons 2 and 3 are depicted as filled and open boxes, respectively. Homology arms are shown as bold lines. Arrowheads show the position and orientation of PCR primers. Triangles flanking the PGK-gb2-neomycin selection cassette (neo) symbolize loxP sequences. **(B)** Southern blot analysis of the genomic DNA from embryonic stem cells using 5' and 3' external probes, as indicated in (A), showed shortening of the diagnostic 22.2-kb-long HindIII fragment present in WT (+/+) down to 9.4 and 13.1 kb, respectively, after homologous recombination (+/neo). **(C)** Cre-mediated deletion of the neomycin selection cassette was confirmed by PCR using forward (F2) and reverse (R2) primers as a shortening of the 2048-bp-long product to 498 bp. neo/neo and -/- represent homozygous animals with targeted loci before and after Cre-mediated deletion of the neomycin selection cassette. **(D)** TLC analysis of neutral GSL isolated from kidneys of WT (+/+) and *Gb3S*-deficient (-/-) mice showed absence of Gb3 and its downstream products such as Gb4. As a consequence, the precursor substance lactosylceramide (LacCer) was increased. As standard (std.), an extract of neutral GSL from human spleen was used. HexCer, hexosylceramide.

FIGURE 3. HPLC analysis of thymi demonstrated the presence of minute amounts of iGb3 in $\alpha\text{GalA}^{-/-}/\text{Gb3S}^{-/-}$ mice. Single-cell suspensions were prepared from murine thymi. After the cell number was determined, homogenates were processed for HPLC. **(A)** In both heterozygous controls and $\text{Gb3S}^{-/-}$ mice, iGb3 was undetectable in thymus. **(B)** The presence of iGb3 could be documented in thymi of $\alpha\text{GalA}^{-/-}/\text{Gb3S}^{-/-}$ mice, which accumulated only isoglobosides but no globosides. **(C)** The iGb3 peak was fully susceptible to α -galactosidase digestion. In contrast, the peak comigrating with Gb3 was unsusceptible to α -galactosidase digestion. **(D)** The iGb3 peak was absent in $\alpha\text{GalA}^{-/-}/\text{Gb3S}^{-/-}/\text{iGb3S}^{-/-}$ triple-knockout mice.



1619 ± 380 molecules of iGb3 per thymocyte (mean \pm SEM, $n = 3$) in this genetically manipulated cross.

iGb3S^{-/-} mice express a typical iNKT TCR repertoire

Previously, we have shown that *iGb3S*^{-/-} mice backcrossed for four generations to the C57BL/6 genetic background had normal iNKT cell frequencies (32). These results could now be verified after further backcrossing of the *iGb3S*^{-/-} mice for >10 generations to the C57BL/6 genetic background (data not shown). Given the normal numbers of iNKT cells in iGb3-deficient mice, we hypothesized that the absence of iGb3 during the process of positive selection might still be reflected by a change in the CDR3 regions of their TCR α - and β -chains. To test this hypothesis, mRNA was isolated from enriched thymic iNKT cells of *iGb3S*^{-/-} and control (*iGb3S*^{+/-}) mice. V α 14 chains were amplified by PCR using V α 14 and C α constant regions primers. The canonical iNKT V α 14-J α 18 CDR3 sequence was dominant in both *iGb3S*^{-/-} (22 of 23 sequences) and control mice (17 of 18) sequences (Fig. 4A). In each case, only one variant was seen, which differed by a single amino acid at the same position. In the case of *iGb3S*^{-/-}, the variant has been previously reported in the iNKT repertoire of WT C57BL/6 mice (4). Murine iNKT cells use V β 2, 7 and 8.2 in combination

with the canonical V α 14-J α 18 α -chain. These TCR β -chains were amplified by PCR using V β -specific primers in combination with C β or, to analyze smaller components of the repertoire, with J β -specific primers. Spectratyping of the PCR products showed highly similar CDR3 length distributions for *iGb3S*^{-/-} and control iNKT cells (Fig. 4B; data not shown). Finally, sequencing of V β 8.2 CDR3 regions showed similar J β segment use (Fig. 4C) and CDR3 diversity (data not shown) within *iGb3S*^{-/-} and control iNKT cells. Overall, these data are consistent with iGb3 presence or absence having minimal impact on the iNKT TCR repertoire, although a minor role for iGb3 in shaping TCR β CDR3 composition cannot be excluded.

Absence of globosides and subgroups of gangliosides did not influence iNKT cell numbers

In view of the fact that Gb3, in contrary to iGb3, is abundantly present in human, mouse, and rat tissues and was also found in lipid eluates from soluble murine CD1d (25), we tested whether the absence of Gb3 would impact iNKT cell development. However, depletion of globosides either alone or in combination with isoglobosides did not alter the frequency of iNKT cells in the thymus, spleen, or liver (Supplemental Fig. 1A). Similarly, depletion of subgroups of gangliosides in mice deficient in GM3-synthase (*GM3S*), GD3-synthase (*GD3S*), and GalNAc-transferase (*GalNAcT*) had no effect on the iNKT cell population (Supplemental Fig. 1B).

Absence of globosides but not of isoglobosides was able to revert the iNKT cell phenotype of $\alpha\text{GalA}^{-/-}$ storage mice

It has been suggested by Darmon et al. (40) that the lowered numbers of iNKT cells in $\alpha\text{GalA}^{-/-}$ mice may be due to the accumulating iGb3, which, by overstimulation of iNKT cells, would lead to their apoptosis. We tested this hypothesis directly by crossing the $\alpha\text{GalA}^{-/-}$ storage mice with *iGb3S*^{-/-} mice. In case that the accumulation of iGb3 would be indeed responsible for the lowered iNKT cell numbers in $\alpha\text{GalA}^{-/-}$ mice, then iNKT cell numbers would be expected to return to WT levels in the $\alpha\text{GalA}^{-/-}/\text{iGb3S}^{-/-}$ double-knockout mice.

In line with previous reports, $\alpha\text{GalA}^{-/-}$ mice showed a significant reduction of the iNKT cell populations both in spleen and liver in comparison with WT mice (Fig. 5A). In the thymus, this reduction reached statistical significance in terms of absolute iNKT cell numbers. However, in $\alpha\text{GalA}^{-/-}/\text{iGb3S}^{-/-}$ mice, iNKT cell numbers were reduced to the same extent as in $\alpha\text{GalA}^{-/-}$ mice (Fig. 5A). In contrast, normalization of the iNKT cell numbers to levels indistinguishable from those in WT mice

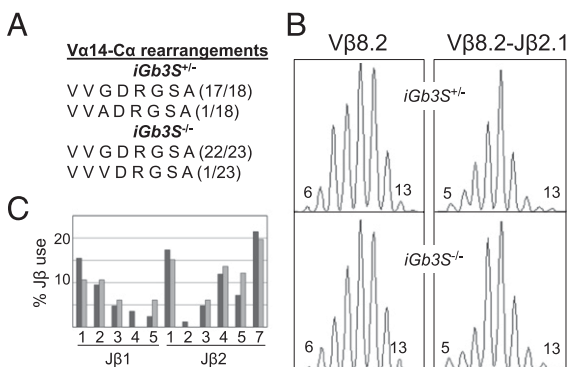


FIGURE 4. *iGb3S*^{-/-} mice expressed a typical iNKT TCR repertoire. iNKT thymocytes from *iGb3S*^{-/-} and control (*iGb3S*^{+/-}) mice were analyzed for TCR usage. **(A)** The canonical iNKT V α 14-J α 18 CDR3 sequence was dominant in *iGb3S*^{-/-} and control mice. **(B)** Total V β 8.2 (left plots) and V β 8.2-J β 2.1 (right plots) TCRs in *iGb3S*^{-/-} (lower plots) and control mice (upper plots) had highly similar CDR3 size distribution spectratypes. CDR3 lengths are indicated. **(C)** Proportional J β segment use within V β 8.2 CDR3 regions of iNKT cells was conserved in the absence of iGb3. Darker and lighter columns are iGb3-deficient and control samples, respectively. Only functional J β gene segments are shown.

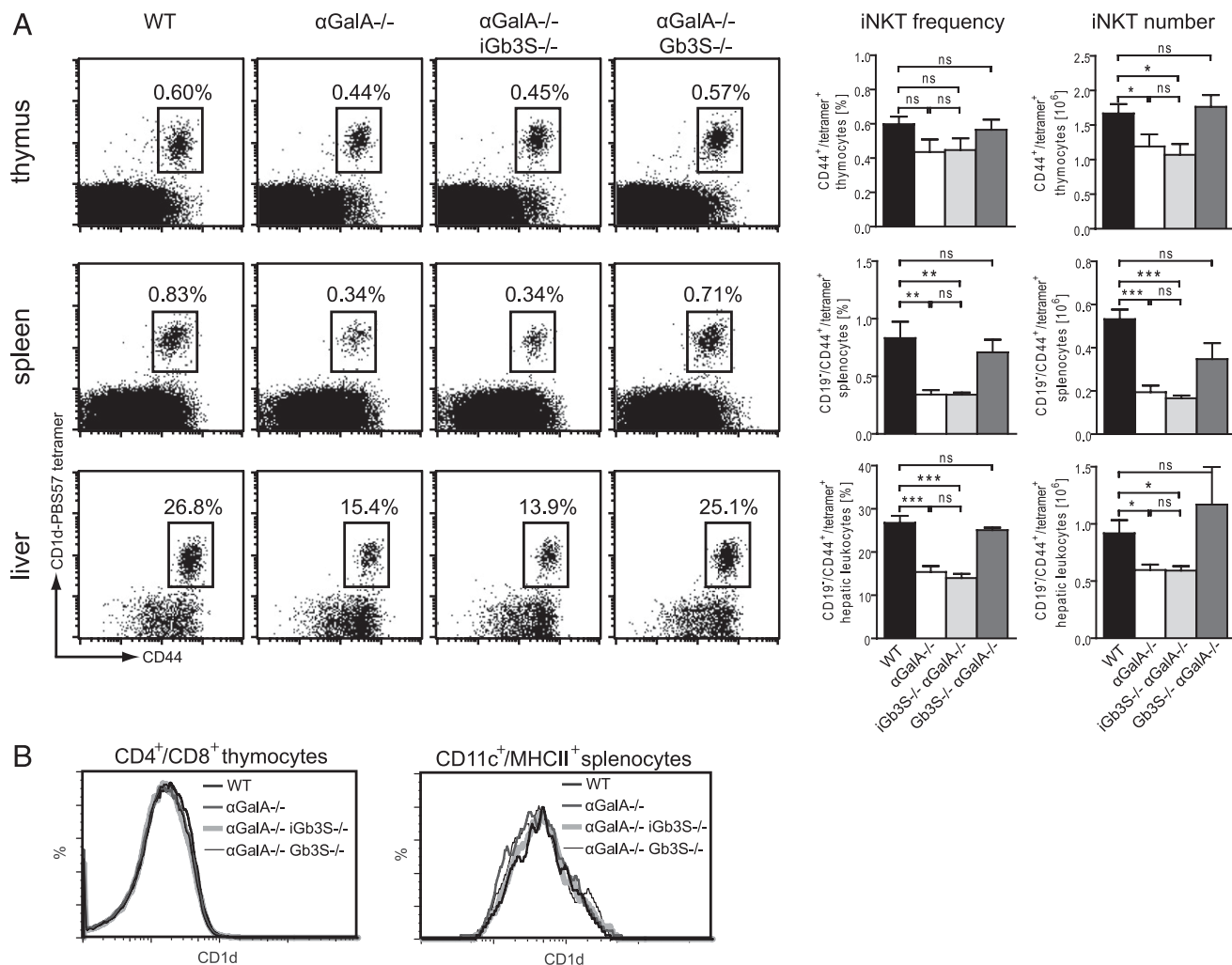


FIGURE 5. iNKT cell phenotype of α GalA^{-/-} storage mice could be reverted by the absence of globosides but not by the absence of isoglobosides. **(A)** Frequencies and absolute numbers of iNKT cells were measured by flow cytometry in 26-wk-old WT, α GalA^{-/-}, α GalA^{-/-}/iGb3S^{-/-}, and α GalA^{-/-}/Gb3S^{-/-} mice using PBS57-loaded CD1d tetramers and anti-CD44 Abs. In the cases of spleen and liver, CD19⁺ cells were gated out. In α GalA^{-/-} storage mice, the iNKT cell population showed a significant reduction in spleens and livers in both relative and absolute numbers; in thymi, the reduction was statistically significant only for absolute iNKT cell numbers. In α GalA^{-/-}/iGb3S^{-/-} mice, the additional iGb3S deficiency did not influence this phenotype. In contrast, in α GalA^{-/-}/Gb3S^{-/-} mice, the absence of globosides restored iNKT cell numbers to WT levels. Bars, means \pm SEM; $n = 6$ –8/group. * $p < 0.05$, ** $p < 0.01$, *** $p < 0.001$. **(B)** Neither of the genotypes influenced CD1d expression on double-positive (CD4⁺/CD8⁺) thymocytes and splenic DCs (CD11c⁺/MHCII⁺) as analyzed by flow cytometry.

could be achieved by depletion of globosides in α GalA^{-/-}/Gb3S^{-/-} mice (Fig. 5A). The expression of CD1d on double-positive (CD4⁺/CD8⁺) thymocytes or splenic DCs (CD11c⁺/MHCII⁺) did not differ from WT in any of these genotypes (Fig. 5B).

The normalization of iNKT cell number in α GalA^{-/-}/Gb3S^{-/-} but not in α GalA^{-/-}/iGb3S^{-/-} mice suggested that the storage of globosides, rather than the accumulation of iGb3, is responsible for the reduction of iNKT cells in α GalA^{-/-} mice. To prove this, we performed further biochemical analyses of spleen tissue from these mice. In parallel, we also analyzed kidneys in which globosides and galabiosylceramide (Gal₂Cer, another Gb3S-dependent GSL; Fig. 1) is present. As expected, accumulation of Gb3 and Gal₂Cer was detected in spleens and kidneys of α GalA^{-/-} mice (Fig. 6A, 6B). Deletion of iGb3S did not alter either the amount or composition of GSL stored in α GalA^{-/-}/iGb3S^{-/-} mice. In contrast, in α GalA^{-/-}/Gb3S^{-/-} mice, deletion of Gb3S abolished the accumulation of GSL (Fig. 6A, 6B). Comparison of the GSL patterns between α GalA^{-/-}/iGb3S^{-/-} and Gb3S^{-/-} mice demonstrated that no GSL other than those dependent on Gb3S

accumulated in α GalA^{-/-}/Gb3S^{-/-} (and α GalA^{-/-}) spleens and kidneys, as detected by TLC (Fig. 6A, 6B).

Electron microscopy further revealed that in α GalA^{-/-} splenocytes accumulation of GSL led to a severe disturbance of lysosomal morphology with numerous enlarged lysosomes filled with lamellar inclusions (Fig. 6C). In line with the TLC findings (Fig. 6A, 6B), this alteration was found also in α GalA^{-/-}/iGb3S^{-/-} but not in α GalA^{-/-}/Gb3S^{-/-} splenocytes (Fig. 6C).

In α GalA^{-/-} splenocytes, GSL storage led to severe impairment of Ag presentation independently of the presence of isoglobosides

On the basis of the severe structural derangement in α GalA^{-/-} splenocytes (Fig. 6C), we speculated that an impairment of Ag presentation caused by lysosomal storage could be the reason for decreased iNKT cell numbers in spleens and livers of these mice. To this end, we have tested the Ag-presenting capacity of DCs enriched from spleens. DCs from α GalA^{-/-} and α GalA^{-/-}/iGb3S^{-/-} were also affected by the storage of Gb3, as shown by flow cytometry with anti-Gb3 Abs (Fig. 7A). The ability of DCs

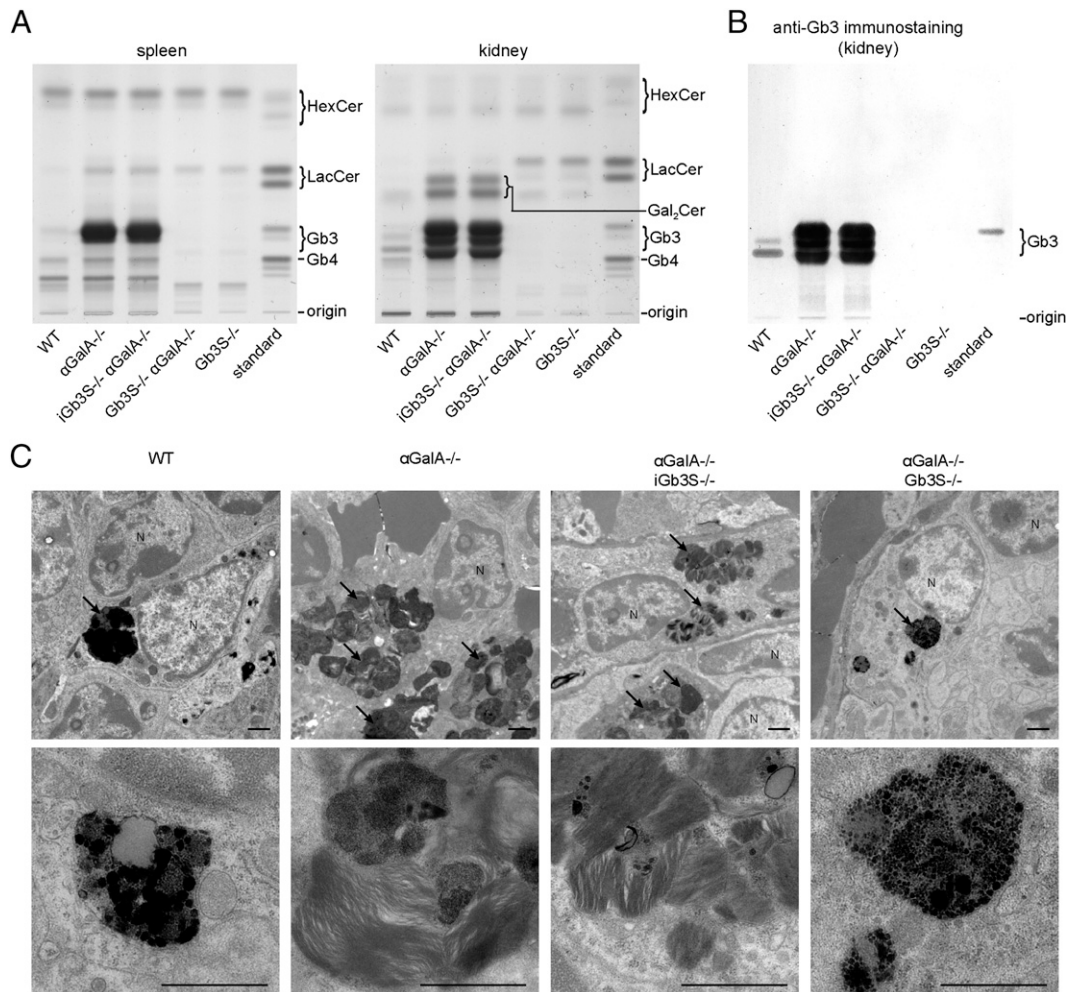


FIGURE 6. Globosides were the major GSL stored in $\alpha\text{GalA}^{-/-}$ splenocytes leading to a severe lysosomal derangement. **(A)** TLC analysis of neutral GSL from spleens and kidneys of WT, $\alpha\text{GalA}^{-/-}$, $\alpha\text{GalA}^{-/-}/i\text{Gb}3\text{S}^{-/-}$, $\alpha\text{GalA}^{-/-}/\text{Gb}3\text{S}^{-/-}$, and $\text{Gb}3\text{S}^{-/-}$ mice. In the spleens and kidneys of $\alpha\text{GalA}^{-/-}$ storage mice, the major accumulating GSL run at the height of Gb3. Additional deficiency for iGb3S did not affect the composition of neutral GSL in $\alpha\text{GalA}^{-/-}/i\text{Gb}3\text{S}^{-/-}$ mice. In contrast, in $\alpha\text{GalA}^{-/-}/\text{Gb}3\text{S}^{-/-}$ mice, the accumulation of globosides (and galabiosylceramide, Gal₂Cer, in kidney) was absent. An extract of neutral GSL from human spleen was used as a standard and orcinol staining was performed for visualization. Heterogeneity in the composition of fatty acid moieties results in some GSL (e.g., Gb3) running as multiple bands (74). **(B)** A TLC plate with renal neutral GSL, which was run in parallel with the one shown in (A), was immunostained with polyclonal Gb3-specific Ab JM06/298-1 (56), which identified the majority of the GSL stored in $\alpha\text{GalA}^{-/-}$ and $\alpha\text{GalA}^{-/-}/i\text{Gb}3\text{S}^{-/-}$ mice to be Gb3. **(C)** Splenic white pulp of 26-wk-old mice was analyzed by transmission electron microscopy. WT splenocytes showed a regular morphology of lysosomes (arrows). In contrast, splenocytes of $\alpha\text{GalA}^{-/-}$ mice were characterized by severely distorted lysosomal architecture with multiple enlarged lysosomes containing abundant lamellar inclusions. This was the case also when isoglobosides were depleted in $\alpha\text{GalA}^{-/-}/i\text{Gb}3\text{S}^{-/-}$ mice. However, in $\alpha\text{GalA}^{-/-}/\text{Gb}3\text{S}^{-/-}$ mice, the depletion of globosides restored the lysosomal architecture to a state morphologically indistinguishable from WT. Scale bar, 1 μm . N, Nucleus.

from $\alpha\text{GalA}^{-/-}$ and $\alpha\text{GalA}^{-/-}/i\text{Gb}3\text{S}^{-/-}$ mice to present the exogenous iNKT cell Ag αGalCer was significantly reduced in comparison with WT mice (Fig. 7B). However, counteracting the storage by depletion of globosides restored the Ag-presenting capacity of $\alpha\text{GalA}^{-/-}/\text{Gb}3\text{S}^{-/-}$ DCs (Fig. 7B). iNKT cell activation by DCs that had been pre-exposed to heat-killed *E. coli* was also substantially diminished in DCs with a storage phenotype, independently of the presence of iGb3S (i.e., in $\alpha\text{GalA}^{-/-}$ and $\alpha\text{GalA}^{-/-}/i\text{Gb}3\text{S}^{-/-}$ DCs (Fig. 7C)). Reversal of storage by depletion of globosides restored microbial activation of iNKT cells to WT levels. Despite the fact that iGb3 has been postulated to mediate iNKT cell activation by DCs upon infection (39), we did not detect any decrease of this interaction when coincubating iNKT cells and $i\text{Gb}3\text{S}^{-/-}$ DCs pre-exposed to heat-killed *E. coli* (Fig. 7C). Furthermore, processing and (cross)-presentation of OVA to peptide-specific T cells was also compromised in a similar manner in $\alpha\text{GalA}^{-/-}$ and $\alpha\text{GalA}^{-/-}/i\text{Gb}3\text{S}^{-/-}$ but not in $\alpha\text{GalA}^{-/-}/\text{Gb}3\text{S}^{-/-}$ DCs (Fig.

7D). Taken together, these results suggest that the storage of globosides leads to a functional alteration in the lysosomal compartment of DCs and subsequent impairment of Ag presentation.

Cholesterol overload induced by AcLDL similarly affected Ag presentation

It has been shown that GSL storage leads to intracellular cholesterol accumulation (57, 58). We hypothesized that cholesterol/cholesteryl ester overload might be one mechanism responsible for the disturbed Ag presentation in $\alpha\text{GalA}^{-/-}$ (and also in $\alpha\text{GalA}^{-/-}/i\text{Gb}3\text{S}^{-/-}$) DCs. To test this, we induced cholesterol overload by exogenous administration of acLDLs to WT BMDCs and investigated their Ag presentation capacity. Cellular lipid accumulation could be documented by Oil Red O stain (Supplemental Fig. 2A) and caused a significant decrease both in αGalCer presentation and in OVA presentation and cross-presentation (Supplemental Fig. 2B, 2C).

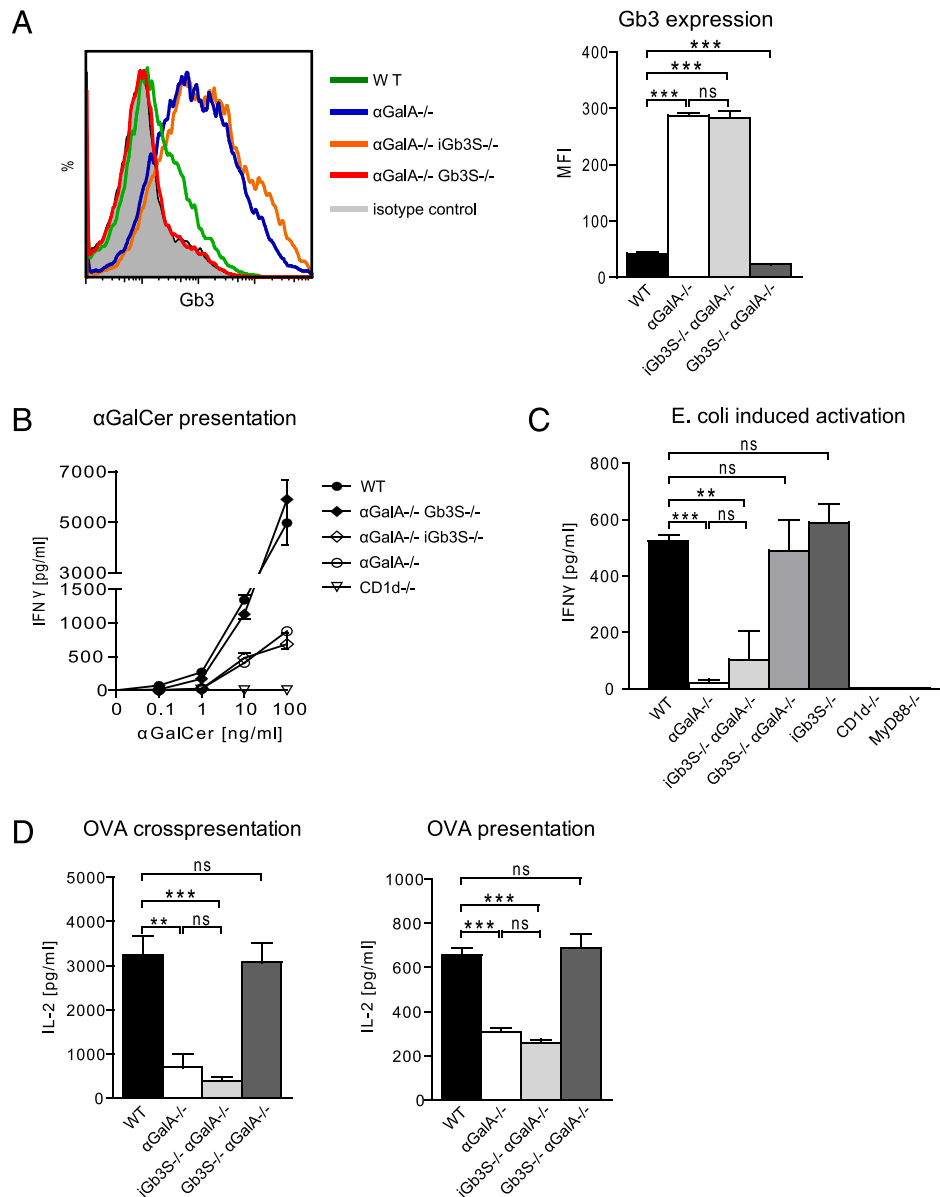


FIGURE 7. DCs from α GalA^{-/-} mice showed a profound defect in Ag presentation including a weaker induction of antimicrobial response by iNKT cells. **(A)** Splenic DCs (enriched by anti-CD11c magnetic beads), which were used for all further experiments, were stained with rat monoclonal IgM anti-Gb3 primary Ab (clone 38-13) in combination with FITC-labeled anti-rat IgM secondary Ab. Flow cytometry demonstrated that Gb3 was expressed at low levels in WT but accumulated extensively in α GalA^{-/-} DCs. This accumulation was absent in α GalA^{-/-}/Gb3S^{-/-} but not in α GalA^{-/-}/iGb3S^{-/-} DCs. Bars, means \pm SEM; $n = 3$ /group. **(B)** In splenic DCs, Ag presentation by CD1d was assessed by exposure to different α GalCer concentrations, followed by coincubation with WT iNKT cells. Presentation of α GalCer on α GalA^{-/-} DCs was significantly diminished throughout the whole range of concentrations tested. Similarly, α GalA^{-/-}/iGb3S^{-/-} DCs showed an impaired α GalCer presentation. This derangement could be returned to normal after depleting the stored globosides in α GalA^{-/-}/Gb3S^{-/-} DCs. CD1d^{-/-} DCs served as negative controls. Shown are means \pm SEM; $n = 4$ /group. **(C)** DC-mediated microbial activation of iNKT cells was tested by applying heat-killed *E. coli* to DCs, followed by coincubation with WT iNKT cells. As for α GalCer, the activation capacity of α GalA^{-/-} and α GalA^{-/-}/iGb3S^{-/-} DCs was significantly lower in comparison with WT, and only the abrogation of storage could restore normal function in α GalA^{-/-}/Gb3S^{-/-} DCs. In iGb3S^{-/-} DCs, the microbe-elicited activation of iNKT cells was unaffected. CD1d^{-/-} and MyD88^{-/-} DCs served as negative controls. Bars, means \pm SEM; $n = 4$ /group. **(D)** The ability of splenic DCs to process and (cross)-present OVA was investigated. To this end, OVA-exposed DCs from the indicated phenotypes were allowed to interact with MHC II- or MHC I-restricted WT T cell hybridomas, and supernatant IL-2 was measured. Both Ag presentation and cross-presentation activity was significantly disturbed on α GalA^{-/-} and α GalA^{-/-}/iGb3S^{-/-} DCs in comparison with WT. DCs from α GalA^{-/-}/Gb3S^{-/-} mice showed an unaltered Ag (cross)-presentation activity. Bars, means \pm SEM; $n = 3$ /group. ** $p < 0.01$, *** $p < 0.001$.

Discussion

iGb3 has been proposed to be the endogenous ligand essential for thymic iNKT cell development (31). Although expression of iGb3S mRNA has been repeatedly documented in murine tissues including thymus (51, 59), the presence of iGb3 in murine thymus has remained controversial. This is based mainly on the fact that

iGb3 and Gb3 are isomers differing solely in the glycosidic linkage of the terminal galactose moiety (Fig. 1), which makes a sensitive discrimination between iGb3 and the much more abundant Gb3 technically extremely challenging. Using a highly sensitive HPLC assay, which allowed detection of iGb3 when present at $>1\%$ of the Gb3 level, iGb3 could not be detected in

murine thymus in WT mice (34). In contrast, analyzing murine thymi by electrospray ionization-linear ion trap-mass spectrometry (ESI-LIT-MSⁿ) Li et al. (33) were able to document signals that could be attributed to iGb3 in an iGb3/Gb3 ratio of 0.4%.

To solve this discrepancy, we have generated a *Gb3S*^{-/-} mouse (Fig. 2) enabling us to address the presence of iGb3 in the absence of its isomer Gb3. To further increase the amounts of the putatively present iGb3, we crossed *Gb3S*^{-/-} mice with *αGalA*^{-/-} mice (murine model of Fabry disease, unable to degrade Gb3 and iGb3, resulting in their supraphysiological levels; Fig. 1). This approach allowed us to detect ~1600 molecules of iGb3 per thymocyte in *αGalA*^{-/-}/*Gb3S*^{-/-} mice (Fig. 3), demonstrating that iGb3 can be synthesized in murine thymus although it does not indicate whether iGb3 is present under physiological conditions in this organ. This is because this genotype represents an extreme situation, as *Gb3S* deletion causes an increase of LacCer (Fig. 2D), which is also the substrate for iGb3S, and furthermore, once synthesized, iGb3 cannot be degraded because of *αGalA* deficiency in these mice. In agreement with this, iGb3 has previously not been reported to be detectable in WT thymus using the same method (34) and was also not detectable in *Gb3S*^{-/-} mice (i.e., in the absence of storage (Fig. 3)). Moreover, these findings also lead to the conclusion that *iGb3S* is the only enzyme responsible for iGb3 synthesis because its trace quantities detected in *αGalA*^{-/-}/*Gb3S*^{-/-} mice were absent in *αGalA*^{-/-}/*Gb3S*^{-/-}/*iGb3S*^{-/-} triple-knockout thymocytes, making the existence of an alternative pathway for iGb3 synthesis in mice very unlikely.

The amount of ~1600 molecules of iGb3 per thymocyte in *αGalA*^{-/-}/*Gb3S*^{-/-} mice (and presumably even lower in WT) seems to be low in terms of structural biology. Nevertheless, it might still be enough to mediate a positive selection of iNKT cells because it has been shown that even a single Ag–MHC complex can elicit a response in conventional T cells (60, 61). Therefore, we readdressed the question of whether depletion of these small iGb3 amounts in congenic iGb3-deficient mice would alter the iNKT cell population. However, backcrossing *iGb3S*^{-/-} mice >10 times to the C57BL/6 genetic background still did not result in any alteration in iNKT cell numbers in *iGb3S*^{-/-} as compared with WT mice. We hypothesized that the absence of iGb3 might still be reflected by alterations in the CDR3 region, which is a part of the interface between the iNKT TCR and iGb3 loaded on CD1d molecules (62). However, the CDR3 region of iNKT cells was preserved despite the absence of iGb3 (Fig. 4), further strengthening the conclusion that iGb3 does not function as the decisive endogenous iNKT selecting ligand.

Brennan et al. (41) have recently shown that GlcCer itself (in particular containing the N-acyl chain C_{24:1}) is recognized by iNKT cells and that recognition of GlcCer-loaded CD1d molecules is responsible for activation of iNKT cells by DCs upon recognition of microbial danger signals. It still remains to be elucidated whether GlcCer also plays a role as the endogenous lipid ligand in the process of thymic iNKT cell selection. However, considering GlcCer as the endogenous ligand for iNKT cell selection might be one explanation for the paradox that iNKT cell development remains unaffected by deficiency of particular GSL groups downstream of GlcCer in the biosynthetic pathway (Fig. 1). The in vivo proof of such a hypothesis would be technically very challenging because mice deficient in GlcCer-synthase (GCS, the enzyme responsible for GlcCer synthesis; Fig. 1) die early during embryogenesis, and working with a conditional knockout or GCS inhibitor is associated with residual traces of GlcCer (63, 64). An alternative explanation has been provided by Facciotti et al. (35) who have shown that peroxisome-derived ether-bonded monoalkyl glycerophosphates are important for iNKT cell development.

Interestingly, until now, alterations of the iNKT cell population have been documented only in mouse models in which the degradation but not the synthesis of GSLs was blocked. The mechanistic basis for this has been controversial. On the basis of the finding that iGb3 stimulated iNKT cells in vitro, Zhou et al. (31) attributed the decreased iNKT cell numbers in *Hexb*^{-/-} mice to decreased lysosomal iGb3 levels because these mice cannot degrade iGb4 to iGb3 (Fig. 1). However, a decrease in the iNKT cell population has been documented in multiple other mouse models of lysosomal GSL storage disease (including *αGalA*^{-/-} mice) irrespective of the specific genetic defect or lipid stored (65, 66). Darmono et al. (40) have suggested that in *αGalA*^{-/-} mice the linking mechanism might be an overstimulation and increased apoptosis of iNKT cells because of iGb3 accumulation, although the accumulation or presence of iGb3 has not been addressed directly. If iGb3 storage would indeed mediate the iNKT cell phenotype in *αGalA*^{-/-} mice, then in *αGalA*^{-/-}/*iGb3S*^{-/-} mice the alterations would be predicted to return to normal. Contrary to this hypothesis, we demonstrate that iNKT cell numbers are decreased to the same extent in *αGalA*^{-/-} and *αGalA*^{-/-}/*iGb3S*^{-/-} mice (Fig. 5), thus implicating strongly that iGb3 cannot be the explanation for the diminished iNKT cell numbers in *αGalA*^{-/-} mice. Moreover, we have found a significant general reduction in the Ag-presenting capacity of *αGalA*^{-/-} and *αGalA*^{-/-}/*iGb3S*^{-/-} splenic DCs (Fig. 7) and reason, in line with a previous publication (65), that all these phenomena are a consequence of storage per se. To prove this, we have performed ultrastructural and biochemical analysis of spleens and documented an accumulation and derangement of lysosomal morphology in both *αGalA*^{-/-} and *αGalA*^{-/-}/*iGb3S*^{-/-} mice (Fig. 6). On TLC, the pattern of accumulated GSL remained identical in *αGalA*^{-/-} and *αGalA*^{-/-}/*iGb3S*^{-/-} mice, with the major contributor to the storage being Gb3 (Fig. 6). Thus, to provide conclusive evidence that storage—and not the accumulation of iGb3—is the real reason for all the morphological and physiological derangements in the function of *αGalA*^{-/-} DCs, we have crossed these mice with *Gb3S*^{-/-} and demonstrated that *αGalA*^{-/-}/*Gb3S*^{-/-} mice, which are devoid of storage (Fig. 6), do not show any functional disturbance in Ag presentation or thymic selection of iNKT cells (Figs. 5, 7). In this context, it is interesting to note that recently Macedo et al. (67) reported that *αGalA* enzyme replacement corrected the iNKT cell deficiency in *αGalA*^{-/-} mice; however, this approach does not allow to discriminate between the effects of the storage of globosides and isoglobosides.

Previous studies have shown that cellular GSL storage may promote cholesterol accumulation (58, 68). Supporting evidence has been published by Glaros et al. (57) demonstrating that apolipoprotein A-I-mediated cholesterol efflux was inhibited in fibroblasts treated with lactosylceramide or a specific glucocerebrosidase inhibitor as well as in fibroblasts from patients with genetic GSL storage diseases (including *αGalA* deficiency). First indications that cholesterol metabolism may influence iNKT homeostasis were provided by Gadola et al. (65) who showed decreased iNKT cell numbers and a defect in *αGalCer* presentation in the murine model for Niemann–Pick disease type C1. Keeping in mind that Niemann–Pick disease type C1 mice store not only cholesterol but also GSL, we tested whether the storage of cholesterol itself can impede Ag presentation and could show that in WT BMDCs cholesterol overload by AcLDL could hinder the presentation of peptide and lipid Ags (Supplemental Fig. 2) similarly to the phenotype seen in *αGalA*^{-/-} and *αGalA*^{-/-}/*iGb3S*^{-/-} mice (Fig. 7). This is congruent with several other findings that imply that hypercholesterolemia and the presence of modified lipoproteins adversely affect the function of APCs (69–71), al-

though no difference in OVA presentation between unloaded and AcLDL-loaded BMDCs was observed by Packard et al. (72). On the basis of our results, we suggest that the cholesterol accumulation that accompanies GSL storage diseases may be one mechanism responsible for the described malfunctioning Ag presentation in $\alpha\text{GalA}^{-/-}$ and $\alpha\text{GalA}^{-/-}/\text{iGb3S}^{-/-}$ mice.

Upon exposure to heat-killed *E. coli*, DCs from $\alpha\text{GalA}^{-/-}$ and $\alpha\text{GalA}^{-/-}/\text{iGb3S}^{-/-}$ mice showed a reduced stimulatory capacity toward iNKT cells in comparison with WT DCs. In contrast, in $\alpha\text{GalA}^{-/-}/\text{iGb3S}^{-/-}$ DCs, the iNKT cell stimulation remained indistinguishable from WT (Fig. 7C). Notably, there was no difference between WT and iGb3-deficient DCs in their iNKT cell stimulatory capacity upon exposure to heat-killed *E. coli* (Fig. 7C). This is in line with our previous results demonstrating that iGb3-deficient myeloid-derived suppressor cells can activate iNKT cells after TLR stimulation (73). Also, injection of iGb3, even at a 10-fold higher dose than αGalCer , did not elicit measurable IFN- γ and IL-4 levels in vivo (data not shown).

Altogether, these results indicate that iGb3, despite its presence in the thymus and its ability to weakly activate iNKT cells in vitro, is unlikely to play a major role in vivo during positive selection of iNKT cells in the thymus or to modulate TLR-mediated crosstalk between DCs and iNKT cells in the periphery. Instead, using a direct genetic approach these results demonstrate that as a consequence of lipid storage, the interaction of DCs and iNKT cells is disturbed irrespective of iGb3 accumulation or lack thereof and provide further evidence that this interaction is not mediated by iGb3.

Acknowledgments

We thank F. van der Hoeven and U. Kloz for blastocyst microinjection, S. Kaden for excellent technical assistance (all at the German Cancer Research Center, Heidelberg, Germany), the National Institutes of Health Tetramer Core Facility at Emory University, Atlanta, GA, for providing PBS57-loaded CD1d tetramers, A. Kulkarni for providing $\alpha\text{GalA}^{-/-}$ mice, and R.L. Proia for providing mice deficient for GalNAc-transferase, GM3-synthase, and GD3-synthase.

Disclosures

The authors have no financial conflicts of interest.

References

- Makino, Y., R. Kanno, T. Ito, K. Higashino, and M. Taniguchi. 1995. Predominant expression of invariant V α 14⁺ TCR α chain in NK1.1⁺ T cell populations. *Int. Immunol.* 7: 1157–1161.
- Arase, H., N. Arase, K. Ogasawara, R. A. Good, and K. Onoé. 1992. An NK1.1⁺ CD4⁺8⁺ single-positive thymocyte subpopulation that expresses a highly skewed T-cell antigen receptor V β family. *Proc. Natl. Acad. Sci. USA* 89: 6506–6510.
- Kronenberg, M., and L. Gapin. 2002. The unconventional lifestyle of NKT cells. *Nat. Rev. Immunol.* 2: 557–568.
- Lantz, O., and A. Bendelac. 1994. An invariant T cell receptor α chain is used by a unique subset of major histocompatibility complex class I-specific CD4⁺ and CD4⁺8⁺ T cells in mice and humans. *J. Exp. Med.* 180: 1097–1106.
- Lee, P. T., K. Benlagha, L. Teyton, and A. Bendelac. 2002. Distinct functional lineages of human V α 24 natural killer T cells. *J. Exp. Med.* 195: 637–641.
- Brigl, M., and M. B. Brenner. 2004. CD1: antigen presentation and T cell function. *Annu. Rev. Immunol.* 22: 817–890.
- Hansen, D. S., and L. Schofield. 2004. Regulation of immunity and pathogenesis in infectious diseases by CD1d-restricted NKT cells. *Int. J. Parasitol.* 34: 15–25.
- Taniguchi, M., M. Harada, S. Kojo, T. Nakayama, and H. Wakao. 2003. The regulatory role of V α 14 NKT cells in innate and acquired immune response. *Annu. Rev. Immunol.* 21: 483–513.
- Van Kaer, L., V. V. Parekh, and L. Wu. 2011. Invariant natural killer T cells: bridging innate and adaptive immunity. *Cell Tissue Res.* 343: 43–55.
- Shimoda, S., K. Tsuneyama, K. Kikuchi, K. Harada, Y. Nakanuma, M. Nakamura, H. Ishibashi, S. Hisamoto, H. Niuro, P. S. Leung, et al. 2012. The role of natural killer (NK) and NK T cells in the loss of tolerance in murine primary biliary cirrhosis. *Clin. Exp. Immunol.* 168: 279–284.
- Das, R., D. B. Sant'Angelo, and K. E. Nichols. 2010. Transcriptional control of invariant NKT cell development. *Immunol. Rev.* 238: 195–215.
- Salio, M., J. D. Silk, and V. Cerundolo. 2010. Recent advances in processing and presentation of CD1 bound lipid antigens. *Curr. Opin. Immunol.* 22: 81–88.

- Kinjo, Y., and K. Ueno. 2011. iNKT cells in microbial immunity: recognition of microbial glycolipids. *Microbiol. Immunol.* 55: 472–482.
- Kronenberg, M., and Y. Kinjo. 2009. Innate-like recognition of microbes by invariant natural killer T cells. *Curr. Opin. Immunol.* 21: 391–396.
- Kawano, T., J. Cui, Y. Koezuka, I. Toura, Y. Kaneko, K. Motoki, H. Ueno, R. Nakagawa, H. Sato, E. Kondo, et al. 1997. CD1d-restricted and TCR-mediated activation of V α 14 NKT cells by glycosylceramides. *Science* 278: 1626–1629.
- Morita, M., K. Motoki, K. Akimoto, T. Natori, T. Sakai, E. Sawa, K. Yamaji, Y. Koezuka, E. Kobayashi, and H. Fukushima. 1995. Structure-activity relationship of α -galactosylceramides against B16-bearing mice. *J. Med. Chem.* 38: 2176–2187.
- Wei, D. G., S. A. Curran, P. B. Savage, L. Teyton, and A. Bendelac. 2006. Mechanisms imposing the V β bias of V α 14 natural killer T cells and consequences for microbial glycolipid recognition. *J. Exp. Med.* 203: 1197–1207.
- Chiu, Y. H., S. H. Park, K. Benlagha, C. Forestier, J. Jayawardena-Wolf, P. B. Savage, L. Teyton, and A. Bendelac. 2002. Multiple defects in antigen presentation and T cell development by mice expressing cytoplasmic tail-truncated CD1d. *Nat. Immunol.* 3: 55–60.
- Smiley, S. T., M. H. Kaplan, and M. J. Grusby. 1997. Immunoglobulin E production in the absence of interleukin-4-secreting CD1-dependent cells. *Science* 275: 977–979.
- Honey, K., K. Benlagha, C. Beers, K. Forbush, L. Teyton, M. J. Kleijmeer, A. Y. Rudensky, and A. Bendelac. 2002. Thymocyte expression of cathepsin L is essential for NKT cell development. *Nat. Immunol.* 3: 1069–1074.
- Zhou, D., C. Cantu, III, Y. Sagiv, N. Schrantz, A. B. Kulkarni, X. Qi, D. J. Mahuran, C. R. Morales, G. A. Grabowski, K. Benlagha, et al. 2004. Editing of CD1d-bound lipid antigens by endosomal lipid transfer proteins. *Science* 303: 523–527.
- Gapin, L. 2010. iNKT cell autoreactivity: what is 'self' and how is it recognized? *Nat. Rev. Immunol.* 10: 272–277.
- Porcelli, S. A., and R. L. Modlin. 1999. The CD1 system: antigen-presenting molecules for T cell recognition of lipids and glycolipids. *Annu. Rev. Immunol.* 17: 297–329.
- Cox, D., L. Fox, R. Tian, W. Bardet, M. Skaley, D. Mojsilovic, J. Gumperz, and W. Hildebrand. 2009. Determination of cellular lipids bound to human CD1d molecules. *PLoS One* 4: e5325.
- Muindi, K., M. Cernadas, G. F. Watts, L. Royle, D. C. Neville, R. A. Dwek, G. S. Besra, P. M. Rudd, T. D. Butters, and M. B. Brenner. 2010. Activation state and intracellular trafficking contribute to the repertoire of endogenous glycosphingolipids presented by CD1d [Published erratum appears in 2010 *Proc. Natl. Acad. Sci. USA* 107: 6118.] *Proc. Natl. Acad. Sci. USA* 107: 3052–3057.
- Yuan, W., S. J. Kang, J. E. Evans, and P. Cresswell. 2009. Natural lipid ligands associated with human CD1d targeted to different subcellular compartments. *J. Immunol.* 182: 4784–4791.
- Pei, B., A. O. Speak, D. Shepherd, T. Butters, V. Cerundolo, F. M. Platt, and M. Kronenberg. 2011. Diverse endogenous antigens for mouse NKT cells: self-antigens that are not glycosphingolipids. *J. Immunol.* 186: 1348–1360.
- Gumperz, J. E., C. Roy, A. Makowska, D. Lum, M. Sugita, T. Podrebarac, Y. Koezuka, S. A. Porcelli, S. Cardell, M. B. Brenner, and S. M. Behar. 2000. Murine CD1d-restricted T cell recognition of cellular lipids. *Immunity* 12: 211–221.
- Stanic, A. K., A. D. De Silva, J. J. Park, V. Sriram, S. Ichikawa, Y. Hirabayashi, K. Hayakawa, L. Van Kaer, R. R. Brutkiewicz, and S. Joyce. 2003. Defective presentation of the CD1d1-restricted natural V α 14Ja18 NKT lymphocyte antigen caused by β -D-glucosylceramide synthase deficiency. *Proc. Natl. Acad. Sci. USA* 100: 1849–1854.
- Xia, C., Q. Yao, J. Schümann, E. Rossy, W. Chen, L. Zhu, W. Zhang, G. De Libero, and P. G. Wang. 2006. Synthesis and biological evaluation of α -galactosylceramide (KRN7000) and isoglobotrihexosylceramide (iGb3). *Bioorg. Med. Chem. Lett.* 16: 2195–2199.
- Zhou, D., J. Mattner, C. Cantu, III, N. Schrantz, N. Yin, Y. Gao, Y. Sagiv, K. Hudspeth, Y. P. Wu, T. Yamashita, et al. 2004. Lysosomal glycosphingolipid recognition by NKT cells. *Science* 306: 1786–1789.
- Porubsky, S., A. O. Speak, B. Luckow, V. Cerundolo, F. M. Platt, and H. J. Gröne. 2007. Normal development and function of invariant natural killer T cells in mice with isoglobotrihexosylceramide (iGb3) deficiency. *Proc. Natl. Acad. Sci. USA* 104: 5977–5982.
- Li, Y., P. Thapa, D. Hawke, Y. Kondo, K. Furukawa, K. Furukawa, F. F. Hsu, D. Adlercreutz, J. Weadge, M. M. Palcic, et al. 2009. Immunologic glycosphingolipidomics and NKT cell development in mouse thymus. *J. Proteome Res.* 8: 2740–2751.
- Speak, A. O., M. Salio, D. C. Neville, J. Fontaine, D. A. Priestman, N. Platt, T. Heare, T. D. Butters, R. A. Dwek, F. Trottein, et al. 2007. Implications for invariant natural killer T cell ligands due to the restricted presence of isoglobotrihexosylceramide in mammals. *Proc. Natl. Acad. Sci. USA* 104: 5971–5976.
- Facciotti, F., G. S. Ramanjaneyulu, M. Lepore, S. Sansano, M. Cavallari, M. Kistowska, S. Forss-Petter, G. Ni, A. Colone, A. Singhal, et al. 2012. Peroxisome-derived lipids are self antigens that stimulate invariant natural killer T cells in the thymus. *Nat. Immunol.* 13: 474–480.
- Brigl, M., and M. B. Brenner. 2010. How invariant natural killer T cells respond to infection by recognizing microbial or endogenous lipid antigens. *Semin. Immunol.* 22: 79–86.
- Page, C., T. Mallevaey, A. O. Speak, D. Torres, J. Fontaine, K. C. Sheehan, M. Capron, B. Ryffel, C. Faveeuw, M. Leite de Moraes, et al. 2007. Activation of invariant NKT cells by Toll-like receptor 9-stimulated dendritic cells requires type I interferon and charged glycosphingolipids. *Immunity* 27: 597–609.

38. Salio, M., A. O. Speak, D. Shepherd, P. Polzella, P. A. Illarionov, N. Veerapen, G. S. Besra, F. M. Platt, and V. Cerundolo. 2007. Modulation of human natural killer T cell ligands on TLR-mediated antigen-presenting cell activation. *Proc. Natl. Acad. Sci. USA* 104: 20490–20495.
39. Mattner, J., K. L. Debord, N. Ismail, R. D. Goff, C. Cantu, III, D. Zhou, P. Saint-Mezard, V. Wang, Y. Gao, N. Yin, et al. 2005. Exogenous and endogenous glycolipid antigens activate NKT cells during microbial infections. *Nature* 434: 525–529.
40. Darmon, A., S. Teneberg, L. Bouzonville, R. O. Brady, M. Beck, S. H. Kaufmann, and F. Winau. 2010. Lysosomal α -galactosidase controls the generation of self lipid antigens for natural killer T cells. *Immunity* 33: 216–228.
41. Brennan, P. J., R. V. Tatituri, M. Brigl, E. Y. Kim, A. Tuli, J. P. Sanderson, S. D. Gadola, F. F. Hsu, G. S. Besra, and M. B. Brenner. 2011. Invariant natural killer T cells recognize lipid self antigen induced by microbial danger signals. *Nat. Immunol.* 12: 1202–1211.
42. Muyrers, J. P., Y. Zhang, and A. F. Stewart. 2001. Techniques: recombinogenic engineering—new options for cloning and manipulating DNA. *Trends Biochem. Sci.* 26: 325–331.
43. Schwenk, F., U. Baron, and K. Rajewsky. 1995. A cre-transgenic mouse strain for the ubiquitous deletion of loxP-flanked gene segments including deletion in germ cells. *Nucleic Acids Res.* 23: 5080–5081.
44. Sango, K., O. N. Johnson, C. A. Kozak, and R. L. Proia. 1995. β -1,4-N-Acetylgalactosaminyltransferase involved in ganglioside synthesis: cDNA sequence, expression, and chromosome mapping of the mouse gene. *Genomics* 27: 362–365.
45. Yamashita, T., A. Hashiramoto, M. Haluzik, H. Mizukami, S. Beck, A. Norton, M. Kono, S. Tsuji, J. L. Daniotti, N. Werth, et al. 2003. Enhanced insulin sensitivity in mice lacking ganglioside GM3. *Proc. Natl. Acad. Sci. USA* 100: 3445–3449.
46. Kawai, H., M. L. Allende, R. Wada, M. Kono, K. Sango, C. Deng, T. Miyakawa, J. N. Crawley, N. Werth, U. Bierfreund, et al. 2001. Mice expressing only monosialoganglioside GM3 exhibit lethal audiogenic seizures. *J. Biol. Chem.* 276: 6885–6888.
47. Ohshima, T., G. J. Murray, W. D. Swaim, G. Longenecker, J. M. Quirk, C. O. Cardarelli, Y. Sugimoto, I. Pastan, M. M. Gottesman, R. O. Brady, and A. B. Kulkarni. 1997. α -Galactosidase A deficient mice: a model of Fabry disease. *Proc. Natl. Acad. Sci. USA* 94: 2540–2544.
48. Lehuen, A., O. Lantz, L. Beaudoin, V. Laloux, C. Carnaud, A. Bendelac, J. F. Bach, and R. C. Monteiro. 1998. Overexpression of natural killer T cells protects $V\alpha 14$ - $J\alpha 281$ transgenic nonobese diabetic mice against diabetes. *J. Exp. Med.* 188: 1831–1839.
49. Exley, M. A., N. J. Bigley, O. Cheng, A. Shaulov, S. M. Tahir, Q. L. Carter, J. Garcia, C. Wang, K. Patten, H. F. Stills, et al. 2003. Innate immune response to encephalomyocarditis virus infection mediated by CD1d. *Immunology* 110: 519–526.
50. Adachi, O., T. Kawai, K. Takeda, M. Matsumoto, H. Tsutsui, M. Sakagami, K. Nakanishi, and S. Akira. 1998. Targeted disruption of the MyD88 gene results in loss of IL-1- and IL-18-mediated function. *Immunity* 9: 143–150.
51. Porubsky, S., S. Wang, E. Kiss, S. Dehmel, M. Bonrouhi, T. Dorn, B. Luckow, C. Brakebusch, and H. J. Gröne. 2011. Rhoh deficiency reduces peripheral T-cell function and attenuates allogeneic transplant rejection. *Eur. J. Immunol.* 41: 76–88.
52. Malle, E., A. Ibovnik, A. Stienmetz, G. M. Kostner, and W. Sattler. 1994. Identification of glycoprotein IIb as the lipoprotein(a)-binding protein on platelets: lipoprotein(a) binding is independent of an arginyl-glycyl-aspartate tripeptide located in apolipoprotein(a). *Arterioscler. Thromb.* 14: 345–352.
53. Malle, E., L. Hazell, R. Stocker, W. Sattler, H. Esterbauer, and G. Waeg. 1995. Immunologic detection and measurement of hypochlorite-modified LDL with specific monoclonal antibodies. *Arterioscler. Thromb. Vasc. Biol.* 15: 982–989.
54. Chomczynski, P., and N. Sacchi. 1987. Single-step method of RNA isolation by acid guanidinium thiocyanate-phenol-chloroform extraction. *Anal. Biochem.* 162: 156–159.
55. Pannetier, C., M. Cochet, S. Darche, A. Casrouge, M. Zöller, and P. Kourilsky. 1993. The sizes of the CDR3 hypervariable regions of the murine T-cell receptor β chains vary as a function of the recombined germ-line segments. *Proc. Natl. Acad. Sci. USA* 90: 4319–4323.
56. Betz, J., M. Bielaszewska, A. Thies, H. U. Humpf, K. Dreisewerd, H. Karch, K. S. Kim, A. W. Friedrich, and J. Mühling. 2011. Shiga toxin glycosphingolipid receptors in microvascular and macrovascular endothelial cells: differential association with membrane lipid raft microdomains. *J. Lipid Res.* 52: 618–634.
57. Glaros, E. N., W. S. Kim, C. M. Quinn, J. Wong, I. Gelissen, W. Jessup, and B. Garner. 2005. Glycosphingolipid accumulation inhibits cholesterol efflux via the ABCA1/apolipoprotein A-I pathway: 1-phenyl-2-decanoylamino-3-morpholino-1-propanol is a novel cholesterol efflux accelerator. *J. Biol. Chem.* 280: 24515–24523.
58. Puri, V., R. Watanabe, M. Dominguez, X. Sun, C. L. Wheatley, D. L. Marks, and R. E. Pagano. 1999. Cholesterol modulates membrane traffic along the endocytic pathway in sphingolipid-storage diseases. *Nat. Cell Biol.* 1: 386–388.
59. Milland, J., D. Christiansen, B. D. Lazarus, S. G. Taylor, P. X. Xing, and M. S. Sandrin. 2006. The molecular basis for gal α (1,3)gal expression in animals with a deletion of the α 1,3galactosyltransferase gene. *J. Immunol.* 176: 2448–2454.
60. Stone, J. D., A. S. Chervin, and D. M. Kranz. 2009. T-cell receptor binding affinities and kinetics: impact on T-cell activity and specificity. *Immunology* 126: 165–176.
61. Sykulev, Y., M. Joo, I. Vturina, T. J. Tsomides, and H. N. Eisen. 1996. Evidence that a single peptide-MHC complex on a target cell can elicit a cytolytic T cell response. *Immunity* 4: 565–571.
62. Zajonc, D. M., P. B. Savage, A. Bendelac, I. A. Wilson, and L. Teyton. 2008. Crystal structures of mouse CD1d-iGb3 complex and its cognate $V\alpha 14$ T cell receptor suggest a model for dual recognition of foreign and self glycolipids. *J. Mol. Biol.* 377: 1104–1116.
63. Jennemann, R., R. Sandhoff, S. Wang, E. Kiss, N. Gretz, C. Zuliani, A. Martin-Villalba, R. Jäger, H. Schorle, M. Kenzelmann, et al. 2005. Cell-specific deletion of glucosylceramide synthase in brain leads to severe neural defects after birth. *Proc. Natl. Acad. Sci. USA* 102: 12459–12464.
64. Yamashita, T., R. Wada, T. Sasaki, C. Deng, U. Bierfreund, K. Sandhoff, and R. L. Proia. 1999. A vital role for glycosphingolipid synthesis during development and differentiation. *Proc. Natl. Acad. Sci. USA* 96: 9142–9147.
65. Gadola, S. D., J. D. Silk, A. Jeans, P. A. Illarionov, M. Salio, G. S. Besra, R. Dwek, T. D. Butters, F. M. Platt, and V. Cerundolo. 2006. Impaired selection of invariant natural killer T cells in diverse mouse models of glycosphingolipid lysosomal storage diseases. *J. Exp. Med.* 203: 2293–2303.
66. Sagiv, Y., K. Hudspeth, J. Mattner, N. Schrantz, R. K. Stern, D. Zhou, P. B. Savage, L. Teyton, and A. Bendelac. 2006. Cutting edge: impaired glycosphingolipid trafficking and NKT cell development in mice lacking Niemann-Pick type C1 protein. *J. Immunol.* 177: 26–30.
67. Macedo, M. F., R. Quinta, C. S. Pereira, and M. C. Sa Miranda. 2012. Enzyme replacement therapy partially prevents invariant natural killer T cell deficiency in the Fabry disease mouse model. *Mol. Genet. Metab.* 106: 83–91.
68. Puri, V., J. R. Jefferson, R. D. Singh, C. L. Wheatley, D. L. Marks, and R. E. Pagano. 2003. Sphingolipid storage induces accumulation of intracellular cholesterol by stimulating SREBP-1 cleavage. *J. Biol. Chem.* 278: 20961–20970.
69. de Bont, N., M. G. Netea, P. N. Demacker, I. Verschueren, B. J. Kullberg, K. W. van Dijk, J. W. van der Meer, and A. F. Stalenhoef. 1999. Apolipoprotein E knock-out mice are highly susceptible to endotoxemia and *Klebsiella pneumoniae* infection. *J. Lipid Res.* 40: 680–685.
70. Ludewig, B., M. Jäggi, T. Dumrese, K. Brduscha-Riem, B. Odermatt, H. Hengartner, and R. M. Zinkernagel. 2001. Hypercholesterolemia exacerbates virus-induced immunopathologic liver disease via suppression of antiviral cytotoxic T cell responses. *J. Immunol.* 166: 3369–3376.
71. Shamshiev, A. T., F. Ampenberger, B. Ernst, L. Rohrer, B. J. Marsland, and M. Kopf. 2007. Dyslipidemia inhibits Toll-like receptor-induced activation of CD8 α -negative dendritic cells and protective Th1 type immunity. *J. Exp. Med.* 204: 441–452.
72. Packard, R. R., E. Maganto-García, I. Gotsman, I. Tabas, P. Libby, and A. H. Lichtman. 2008. CD11c⁺ dendritic cells maintain antigen processing, presentation capabilities, and CD4⁺ T-cell priming efficacy under hypercholesterolemic conditions associated with atherosclerosis. *Circ. Res.* 103: 965–973.
73. De Santo, C., M. Salio, S. H. Masri, L. Y. Lee, T. Dong, A. O. Speak, S. Porubsky, S. Booth, N. Veerapen, G. S. Besra, et al. 2008. Invariant NKT cells reduce the immunosuppressive activity of influenza A virus-induced myeloid-derived suppressor cells in mice and humans. *J. Clin. Invest.* 118: 4036–4048.
74. Mühling, J., C. H. Schweppe, H. Karch, and A. W. Friedrich. 2009. Shiga toxins, glycosphingolipid diversity, and endothelial cell injury. *Thromb. Haemost.* 101: 252–264.